Subnanosecond Geminate Charge Recombination in Polymer-Polymer Photovoltaic Devices

Justin M. Hodgkiss,[*,†] Andrew R. Campbell, R. Alex Marsh, Akshay Rao, Sebastian Albert-Seifried, and Richard H. Friend[*]

Cavendish Laboratory, Department of Physics, University of Cambridge, CB3 0HE, United Kingdom

(Received 13 December 2009; published 29 April 2010)

We present direct spectroscopic evidence for substantial subnanosecond charge recombination in polymer-polymer blend photovoltaic devices. Early dynamics are dominated by exciton-charge interactions associated with high initial excitation densities. Independent of density, 30% of charges subsequently recombine geminately within just 2 nanoseconds, in contrast with fullerene blends. The remainder recombines with a half-life of ~200 ns. The morphological invariance of subnanosecond recombination suggests that its origin is inherent in the molecular structure at the polymer-polymer interface.

DOI: 10.1103/PhysRevLett.104.177701 PACS numbers: 84.60.Jt, 78.47.jb, 81.05.Fb, 88.40.jr

Considerable effort is being invested in the development of new materials for use in organic photovoltaic (OPV) devices, with particular emphasis on rationally designing their energy levels [1–4]. Donor-acceptor copolymers with strong charge-transfer absorption bands matched to the solar spectrum are combined with $PC_{71}BM$ ([6,6]-phenyl-C_{71}-butyric acid methyl ester) to create OPVs with the highest power conversion efficiencies to date [1,5,6].

The strong optical absorption of donor-acceptor copolymers and their tunable energy levels also make them attractive candidates as electron acceptors which could facilitate efficient charge transfer without compromising the retained voltage. One promising electron accepting copolymer is F8TBT {poly[(9,9-dioctylfluorene)-2,7-diyl-alt-[4,7-bis(3-hexylthien-5-yl)-2,1,3-benzo-thiadiazole]-2,2-diyl]} [Fig. 1(a)] [2]. F8TBT features a backbone sequence of alternating electron donor [dioctylfluorene (F8)] and acceptor [dithienyl-benzothiadiazole (TBT)] units that produce a strong charge-transfer absorption band in the visible. Its energy levels are suitably positioned to act as either an electron donor (when blended with PCBM) or an electron acceptor (when blended with P3HT). The latter configuration leads to the most efficient polymer-polymer blended photovoltaic device to date [2,7]. As expected, absorption into both polymers contributes significantly to photocurrent generation in P3HT:F8TBT blend devices [7], and higher open-circuit voltages are found ($V_{OC} = 1.2$ V)[2] compared with P3HT : C_{61}PCBM blend devices ($V_{OC} \sim 0.6$ V) [8]. However, the modest external quantum efficiency (EQE) of photocurrent generation limits the overall power conversion efficiency of the polymer-polymer blend to 1.8%. As in other OPV devices, reduced EQEs are taken to reflect the recombination of photogenerated charge pairs on time scales faster than they can be completely separated and extracted [9].

Here, we report the application of transient absorption (TA) spectroscopy to uncover the charge recombination time scales against which photocurrent extraction must compete. After accounting for a density-dependent artifact operating in competition with charge generation on picosecond time scales, we show that the intrinsic charge recombination dynamics are distinctly biphasic; 30% of photogenerated charge pairs recombine within just two nanoseconds, and the remainder recombines with a half-life of approximately 200 ns. The subnanosecond recombination phase is substantially faster than seen in polymer-PCBM blends and represents a challenge to the development of materials for photovoltaics.

P3HT-F8TBT thin films and devices were fabricated and their PV responses tested as previously described [10]. Where required, films were annealed on a hotplate at 140 °C for 10 minutes immediately after spin- coating. TA spectroscopy was carried out using previously described methods [11,12]. For time scales shorter than 2 ns, pulsed excitation was provided by the 500-nm, 60-fs output of an optical parametric amplifier (OPA, topas). Broadband probe pulses were generated in a noncollinear optical parametric amplifier. Special care was taken to ensure that the spatial overlap of excitation and probe beams was maintained throughout the entire range of delay stage translation. High intensity effects associated with pulsed excitation are known to be problematic in TA spectroscopy of thin films [13]. We established that ~50% of excitations are lost via high intensity effects in an annealed film by observing that the EQE of a corresponding device is suppressed by slightly over twofold under identical pulsed excitation conditions compared with the cw limit. TA measurements on longer time scales employed the second harmonic (532 nm, 600 ps) output of a *Q*-switched laser synchronized with the same broadband probe. Samples were contained in a vacuum chamber ($\sim 10^{-5}$ mbar) during TA measurements.

Figure 1 shows TA spectra of thin films of the individual constituent polymers and a thermally annealed blend between 200 fs and 1.2 ns. P3HT [Fig. 1(a)] exhibits positive differential transmission signals across most of the spectrum. Comparison with the ground-state absorption spectrum enables the assignment of a transient ground-state

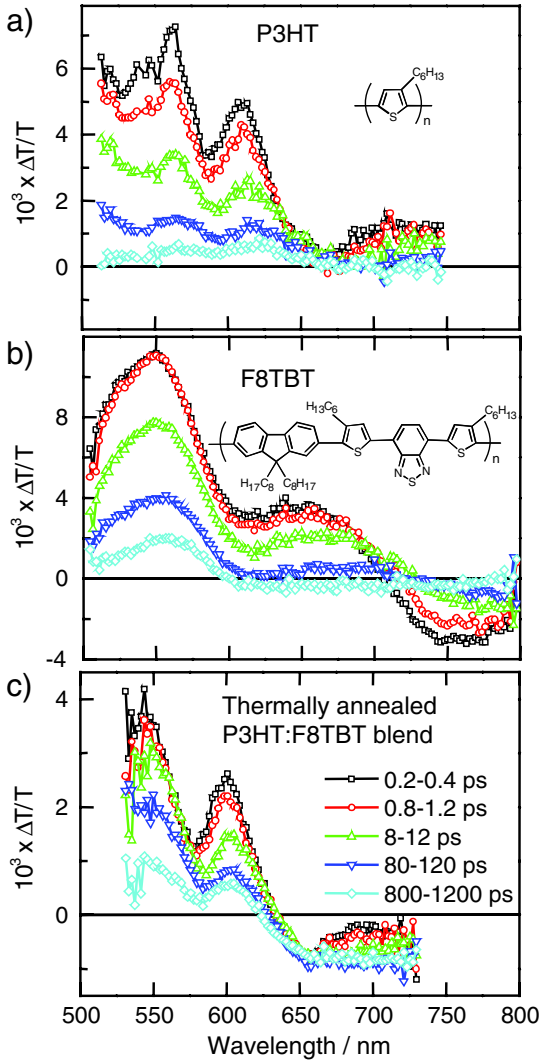

FIG. 1 (color online). TA spectral evolution for thin films of (a) P3HT, (b) F8TBT, and (c) a thermally annealed blend of P3HT and F8TBT following 60-fs, 500 nm pulsed excitation (1×10^{14} photons/cm^2). The integrated time ranges indicated in part (c) also apply to parts (a) and (b). The slightly limited spectral range in parts (a) and (c) reflects the difficulty in consistently generating stable white-light continuum in the 750 nm region.

bleach (GSB) feature with distinct vibronic peaks at 560 nm (0–1) and 610 nm (0-0). Further to the red, the positive peak at ~720 nm corresponds to photoluminescence (PL) from regioregular P3HT, and is thus assigned to stimulated emission (SE) from singlet excitons in the TA spectra. By comparison with the published luminescence lifetime of P3HT ($\tau \sim 500$ ps) [14], exciton decay appears to be accelerated by some degree of exciton annihilation at the fluence used here for TA spectroscopy.

In the case of F8TBT [Fig. 1(b)], the positive differential transmission feature at 550 nm corresponds to bleaching of the charge-transfer absorption band in F8TBT, while the shoulder at 650 nm is attributed to SE from singlet excitons in F8TBT. A photoinduced absorption (PIA) signal is seen within the detection window ($\lambda_{max} = 750$ nm). The PIA decays on the same time scale as the SE signal and is thus also attributed to the singlet exciton. After 1 ns, the excitonic features have clearly decayed; however, nearly 20% of the GSB signal remains. A broad PIA that persists to the red of the GSB implies the direct formation of a population of charges in F8TBT, consistent with previous investigations of a closely related polymer [15].

The TA spectral dynamics of constituent polymers enables us to interpret that of the thermally annealed blend shown in Fig. 1(c). The blend TA spectrum exhibits a distinct difference to those of the individual polymers; even within the first picosecond, the blend exhibits a PIA signal at wavelengths beyond 640 nm. The PIA cannot be attributed to excitations in one or other phase of the blend since neither P3HT nor F8TBT on its own has a PIA signal in the wavelength range of 640–710 nm on this time scale. We therefore attribute the prompt appearance of a PIA signal to charge pairs comprised of electrons occupying F8TBT and holes on the P3HT side of the interface. PIA is initially peaked at around 650 nm in the blend and subsequently evolves to a broad featureless absorption that extends beyond 750 nm on a time scale of 10's of picoseconds. The observed spectral evolution can be explained by a combination of prompt and delayed charge generation. Initially, a broad featureless PIA from promptly formed charge pairs is superimposed with the spectrum of a population of P3HT excitons. P3HT excitons contribute a SE peak that cancels much of the PIA around 700 nm, giving the impression that PIA is peaked at 650 nm. The SE contribution disappears as the remaining excitons diffuse to charge-separating interfaces, leaving a broad PIA feature when only charge pairs remain beyond 100 ps.

Charge generation dynamics in the thermally annealed blend are clearly resolved in the 650–700 nm integrated kinetics shown in Fig. 2(a). The PIA signal attributed to interfacial charge pairs appears within the first 100 fs, suggesting that many excitons are generated on polymer chains that are essentially at a heterojunction interface. The PIA signal grows with a characteristic time scale of a few picoseconds. The maximum PIA signal is reached at approximately 100 ps, beyond which its magnitude decays by approximately 30% within 2 ns. The decaying PIA suggests that a significant proportion of photogenerated charge pairs recombine substantially faster than expected, thus preventing their extraction as photocurrent.

It is plausible that the PIA decay results from a dynamically shifting charge spectrum (i.e., shifting out of our detection window) rather than charge recombination. However, the GSB signal at $\lambda < 640$ nm in the TA spectra applies to all charged and neutral excitations, regardless of where the associated PIA is peaked. Therefore, the magnitude of the GSB signal quantitatively reflects the total population of all excitations, and its decay reflects recovery of the ground state, assuming that all excitations have the same bleaching cross section. On time scales beyond which only charge pairs exist, the GSB decays via charge

recombination. Integrated normalized GSB kinetics for the blend and individual polymers are also shown in Fig. 2(a). In the case of the annealed blend, ground state recovery initially proceeds on a similar time scale as for P3HT excitons. A higher population of excitations survives beyond 100 ps in the blend (as charge pairs) than in P3HT. The GSB decay within the first 100 ps appears to contradict our conclusion from the PIA dynamics that excitons are converted to charge pairs within this time scale since this process would conserve the GSB signal.

The apparent contradiction between PIA and GSB kinetics is resolved by including an exciton annihilation channel at the densities employed for these measurements. The GSB decay in Fig. 2(a) suggests that approximately 50% of excitons are annihilated within 100 ps, preventing them from generating charges and contributing to photocurrent. Considering that the EQE of the corresponding device under identical pulsed excitation conditions is attenuated to slightly under 50% of the cw excitation EQE, this analysis suggests that annihilation within the first 100 ps is the only significant density-dependent recombination channel at the fluence used. Bimolecular charge recombination cannot account for the density-dependent decay within 100 ps because the charge population is peaked at 100 ps. Excitons can be annihilated via long-range Förster transfer to charges at even lower excitation densities than the threshold for exciton-exciton annihilation, owing to strong resonance between exciton emission and charge absorption [12].

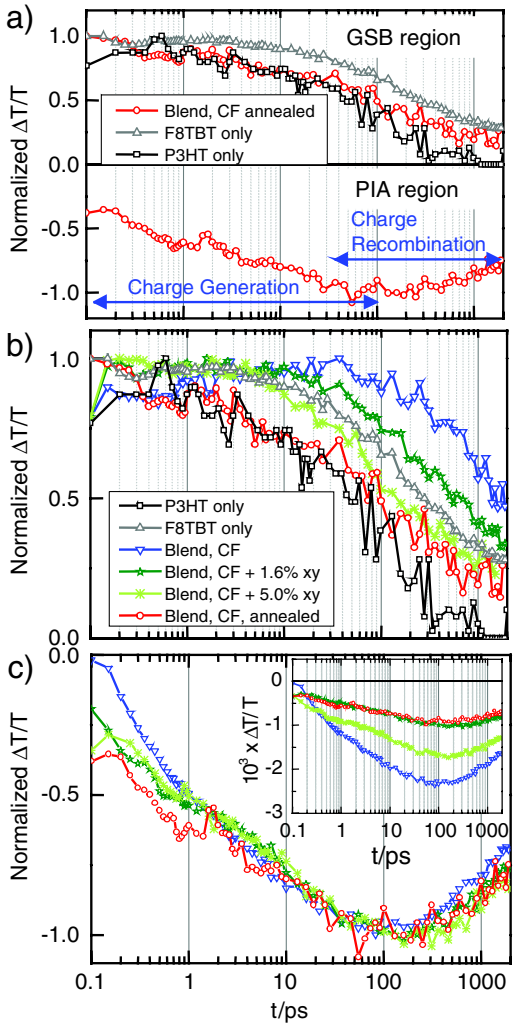

FIG. 2 (color online). (a) TA kinetics for a thermally annealed blend of P3HT and F8TBT in the GSB region (530–570 nm) and the PIA region (650–700 nm) under the same excitation conditions as Fig. 1. GSB kinetics (530–570 nm) for P3HT and F8TBT are also included. (b) GSB kinetics for a series of films with various morphologies controlled by the ratios of chloroform (CF), *p*-xylene (*xy*), or by annealing. (c) Normalized and nonnormalized (inset) PIA kinetics for the same series.

In order to probe the influence of blend morphology, we measured charge generation and recombination dynamics in as-spun films of P3HT:F8TBT from different solvent mixtures. Films cast from chloroform dry rapidly, leaving little opportunity for polymer chains to phase separate or arrange into crystalline lamellae. We have previously shown that addition of a small fraction of a high boiling-point cosolvent controllably slows the rate of film drying, resulting in coarser film morphologies, a higher degree of P3HT crystallinity, and markedly improved EQEs [10]. Figures 2(b) and 2(c) show the kinetics of charge generation and recombination probed in the GSB and PIA regions for films cast from chloroform, with 1.6 and 5% *p*-xylene by volume compared with the thermally annealed film cast from chloroform. The series of GSB decays in Fig. 2(b) are understood in terms of the model described above; diffusion-limited charge generation and exciton-charge annihilation compete with each other within the first 100 ps, following which geminate recombination depletes the charge population. The GSB remains constant for the first 100 ps in the case of the blend cast from chloroform, suggesting quantitative conversion of excitons to charges and the absence of exciton annihilation reactions. As the blend morphology is coarsened via increasing the volume fraction of high boiling-point cosolvent (or via thermal annealing), exciton-charge annihilation becomes competitive since it operates over a longer range than exciton diffusion or charge generation, thus causing additional decay of the GSB signal within 100 ps. The long-range operation of exciton-charge annihilation effectively means that we only resolve charge generation dynamics for those excitons created close to an interface in all morphologies—resulting in little change to the time of peak charge population [~100–200 ps for all morphologies, see Fig. 2(c)]. The inherent half-life for diffusion-limited charge generation can be estimated as approximately 8 ps in the annealed blend, based on the measured 4-ps half-life arising from approximately equal contributions of charge generation and exciton-charge annihilation. The charge generation time scale is substantially faster than the lifetime of excitons in the individual polymers; therefore, inherent exciton decay is not a significant decay channel, and the length scale of phase separation is determined to be smaller

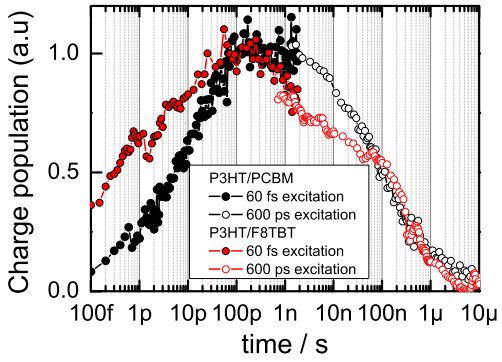

FIG. 3 (color online). Combined charge generation and recombination kinetics for thermally annealed P3HT/F8TBT blend compared with P3HT/PCBM. The short time scale PIA measurement (as described in Fig. 1) is normalized to the peak charge population. Longer time scales were measured with 600 ps, 532 nm excitation (2×10^{13} photons/cm^2), a probe range of 650–750 nm, and normalized to splice to the earlier data at 2 ns.

than exciton diffusion lengths. The magnitude of the peak charge population (see inset of Fig. 2(c) for non-normalized PIA dynamics) is attenuated in coarser blends to an extent commensurate with degree of exciton-charge annihilation.

Exciton-charge annihilation is an artifact of high initial pulsed excitation densities that accounts for the ~50% attenuation in device EQE measured at the same fluence. We therefore determine that the linear density regime is restored on subsequent time scales. In the density regime relevant to PV operation under solar illumination, Fig. 2(c) clearly shows that approximately 30% of charges recombine between 100 ps and 2 ns, independent of blend morphology and peak charge density. The universality of rapid recombination suggests that its origin is inherent to the molecular nature of the donor-acceptor interface rather than the blend morphology. Coupling between various interfacial states involving the alternating donor-acceptor copolymer F8BT has been shown to be extremely sensitive to the molecular configuration at the interface [16]. Other quantum chemical descriptions of heterojunction interfaces allow for a wide range of recombination times owing to molecular level perturbations in electronic energy levels and electronic coupling matrix elements [17,18].

We probed the recombination dynamics of the remaining charges on longer time scales by synchronizing the femtosecond broadband probe pulse with a Q-switched 600 ps, 532 nm excitation laser via an electronic delay generator. When combined with the fast time resolution from mechanical pump-probe delays, we achieve gap-free time resolution over the entire lifetime of photogenerated charges. The combined PIA dynamics in Fig. 3 illustrate distinct temporal regions of charge recombination; 30% of charges recombine between 100 ps and 2 ns; the remaining 70% of charges recombine substantially slower—with a half-life of approximately 200 ns. In an OPV device, complete charge separation and extraction must compete against the recombination kinetics in Fig. 3.

TA measurements on more efficient P3HT-PCBM blend devices with the same experimental setup and excitation conditions reveal recombination dynamics that closely resemble those of P3HT-F8TBT for time scales beyond 2 ns (Fig. 3) [13]. Charge recombination on time scales of tens of nanoseconds has previously been measured for other polymer-fullerene blends, albeit under higher excitation densities [19–21]. However, the subnanosecond recombination phase revealed here for P3HT-F8TBT is absent in polymer-PCBM blends (Fig. 3) [22], representing a substantial loss that appears to be inherent to the polymer-polymer interfacial molecular electronic structure. The ability to circumvent recombination is the subject of considerable research efforts—often via improving morphologies, promoting polymer crystallinity, and enhancing charge mobilities [1,8,10,23]. The occurrence of subnanosecond recombination in P3HT-F8TBT blends suggests that redesigning heterojunction interfaces to facilitate rapid long-range charge separation will be key to realizing efficient polymer-polymer blend OPV devices that retain high open-circuit voltages.

This work was supported by a grant from the U.K. Engineering and Physical Sciences Research Council (EPSRC).

*Justin.Hodgkiss@vuw.ac.nz; rhf10@cam.ac.uk
†Present address: MacDiarmid Institute for Advanced Materials and Nanotechnology, School of Chemical and Physical Sciences, Victoria University of Wellington, New Zealand.

[1] J. Peet *et al.*, Nature Mater. **6**, 497 (2007).
[2] C. R. McNeill *et al.*, Appl. Phys. Lett. **90**, 193506 (2007).
[3] O. Inganäs *et al.*, Appl. Phys. A **79**, 31 (2004).
[4] N. Blouin *et al.*, J. Am. Chem. Soc. **130**, 732 (2008).
[5] J. Hou *et al.*, J. Am. Chem. Soc. **131**, 15586 (2009).
[6] S. H. Park *et al.*, Nat. Photon. **3**, 297 (2009).
[7] C. R. McNeill *et al.*, Adv. Funct. Mater. **19**, 3103 (2009).
[8] W. Ma *et al.*, Adv. Funct. Mater. **15**, 1617 (2005).
[9] M. Lenes *et al.*, Adv. Funct. Mater. **19**, 1106 (2009).
[10] A. R. Campbell *et al.*, Nano Lett. **8**, 3942 (2008).
[11] S. Westenhoff *et al.*, J. Am. Chem. Soc. **130**, 13653 (2008).
[12] J. M. Hodgkiss *et al.*, J. Am. Chem. Soc. **131**, 8913 (2009).
[13] R. A. Marsh, J. M. Hodgkiss, and R. H. Friend, Adv. Mater. (to be published).
[14] J. Clark *et al.*, Phys. Rev. Lett. **98**, 206406 (2007).
[15] M. Westerling *et al.*, Phys. Rev. B **75**, 224306 (2007).
[16] Y.-S. Huang *et al.*, Nature Mater. **7**, 483 (2008).
[17] A. Burquel *et al.*, J. Phys. Chem. A **110**, 3447 (2006).
[18] J.-L. Brédas *et al.*, Acc. Chem. Res. **42**, 1691 (2009).
[19] S. De *et al.*, J. Am. Chem. Soc. **129**, 8466 (2007).
[20] S. J. C. Meskers *et al.*, Phys. Rev. B **61**, 9917 (2000).
[21] T. Offermans, S. C. J. Meskers, R. A. J. Janssen, J. Chem. Phys. **119**, 10924 (2003).
[22] R. A. Marsh *et al.*, Nano Lett. **10**, 923 (2010).
[23] V. D. Mihailetchi *et al.*, Adv. Funct. Mater. **16**, 699 (2006).